



Cite this: *React. Chem. Eng.*, 2019, 4, 27

Continuous-flow liquid-phase dehydrogenation of 1,4-cyclohexanedione in a structured multichannel reactor†

M. Arsalan Ashraf,^a Julia Tan,^a Matthew G. Davidson,^b Steven Bull,^b Marc Hutchby,^b Davide Mattia^a and Pawel Plucinski^{*a}

A highly selective, scalable and continuous-flow process is developed for the liquid-phase dehydrogenation of 1,4-cyclohexanedione to hydroquinone in a millimetre-scale structured multichannel reactor. The square-shaped channels (3 mm × 3 mm) were filled with 10 wt% Pd/C catalyst particles and utilized for the dehydrogenation reaction in single-pass and recycle modes. For the purpose of enhancing process understanding and maximizing conversion and selectivity by process optimization, the design of experiment (DoE) methodology was utilized by studying the effect of operating parameters on the catalytic performance in the kinetic regime. The results demonstrated the strong influence of temperature and liquid feed flow on the conversion and selectivity, with liquid feed and N₂ flows influencing pressure drop significantly. A multi-objective optimization methodology was used to identify the optimum process window with the aid of sweet spot plots, with design space plots developed to establish acceptable boundaries for process parameters. In single-pass mode, complete conversion per pass per channel was not achievable, whereas conversion increased from 59.8% in one channel to 78.3% for two channels in series while maintaining selectivity (>99%) with intermediate hydrogen removal. However, without the intermediate H₂ removal step, selectivity decreased from >99% in one channel to 82.3% at the outlet of the second channel. In recycle mode, the dehydrogenation reaction resulted in almost complete conversion (>99%) with very high selectivity (>99%) and yield (>98%). This combination of mm-scale multichannel reactor and DoE methodology opens the way to developing highly selective and scalable dehydrogenation processes in the fine chemical and pharmaceutical industries.

Received 19th August 2018,
Accepted 31st October 2018

DOI: 10.1039/c8re00176f

rsc.li/reaction-engineering

1. Introduction

Climate change, security of fossil fuel supply and other considerations are driving the development of a biomass-based economy. The existing industrial process routes are developed to synthesize chemicals from fossil feedstock. In turn, the oxygen-rich chemistry of bio-feedstocks requires novel synthetic routes to key chemicals that can be prepared using economical and environmentally viable processes.^{1,2} In the fine chemical and pharmaceutical industries, dehydrogenation is an interesting reaction in the formation of highly valuable ketones, aldehydes and aromatic compounds from renewable feedstock. Endothermic dehydrogenation is usually performed at higher temperature and lower pressure. However, insufficient chemical stability of most fine

chemicals requires the reaction to be performed under moderate conditions in the liquid phase with the use of a solvent. This dehydrogenation to aromatic compounds becomes more complex in terms of achieving high selectivity when a hydroxyl, carbonyl or acid anhydride group is attached to the ring.³

Hydroquinone is a key intermediate (benzene ring with two hydroxyl groups) in the production of many high-value fine chemicals and pharmaceutical ingredients, with hydroquinone currently produced from petroleum-based feedstocks such as benzene, phenol, and aniline.⁴ It has commercial applications such as an antioxidant in skincare products,⁵ as a polymerization inhibitor,⁶ and as a photo-developing agent.⁷ However, hydroquinone can potentially be synthesized by the dehydrogenation of 1,4-cyclohexanedione,⁸ which, in turn, can be derived from bio-renewable succinic esters⁹ that can be accessed from lignocellulosic feedstocks using fermentative processes.¹⁰

In fine-chemical processes, multiphase dehydrogenation of cyclohexanones is currently performed in conventional slurry reactors: for instance, the liquid phase

^a Department of Chemical Engineering, University of Bath, Claverton Down, Bath BA27AY, UK. E-mail: M.A.Ashraf@bath.ac.uk, P.Plucinski@bath.ac.uk

^b Department of Chemistry, University of Bath, Claverton Down, Bath BA27AY, UK

† Electronic supplementary information (ESI) available. See DOI: 10.1039/c8re00176f



The catalytic performance of multiphase dehydrogenation reaction can be assumed as a sequence of fundamental steps: (1) diffusion of 1,4-cyclohexanedione from the liquid feed stream to the surface of the Pd/C particles, (2) subsequent diffusion through the pore network of activated carbon, (3) followed by adsorption on the metallic Pd catalyst surface, (4) then surface reaction leading to the formation of products (*i.e.*, hydroquinone, hydrogen *etc.*), (5) eventually the desorption of the products from the metallic Pd catalyst surface, (6) which diffuse away from the catalyst surface through the pore structure back to the bulk stream. Hydroquinone remains in the liquid phase, whereas the produced hydrogen goes to the surrounding gas stream.

The plug flow behaviour in the mm-scale structured packed bed reactor was confirmed by a number of appropriate criteria, *i.e.*, ratio of reactor to particle diameter, ratio of reactor length to particle diameter, and Peclet number. The presence of external and internal mass transfer diffusion limitations was evaluated under extreme operating conditions at higher conversion (79.1%) for experiment N17 ($T = 240\text{ }^{\circ}\text{C}$, $F_L = 0.1\text{ mL min}^{-1}$, $F_G = 5\text{ mL min}^{-1}$, and $C_o = 10$); see Table S1 in the ESI.†

The understanding of the interaction at the liquid–solid interphase is very important for uniform distribution of the liquid stream surrounding the catalyst particles in heterogeneous multiphase reactors. Small catalyst particles (50–200 μm) in micro/mm-scale packed bed reactors alter the prevailing hydrodynamics of multiphase flow, which is not characteristic of trickle flow regimes, and help to overcome the non-idealities of trickle bed reactors: (1) incomplete wetting, (2) internal concentration gradient, (3) flow maldistribution, and (4) temperature gradient on reactor scale.^{37,38} The small particle size (64.4 μm) results in capillary forces dominating over viscous and gravitational forces, which results in almost complete wetting of the catalyst bed.³⁹ However, further decrease in particle size (<50 μm) will result in a significant pressure drop over the catalyst bed. The dehydrogenation reaction is favoured at lower pressure. The smaller particles and longer channel length will increase the pressure drop significantly, with a negative influence on yield and energy requirements. The Sie criterion⁴⁰ (eqn (1)) was used to estimate the wetting characteristics of the catalyst packed bed.

$$\frac{(dP/dh)_{\text{flow}}}{(dP/dh)_{\text{gravity}}} = \frac{180\mu_L u_L (1-h_L \varepsilon_b)^2}{h_L \varepsilon_b d_p^2 \rho_L g (h_L \varepsilon_b)^3} > 1 \quad (1)$$

where g is the gravitational constant (9.81 m s^{-2}), μ_L is the feed mixture viscosity (Pa s), ρ_L is the feed mixture density (kg m^{-3}), ε_b is the catalyst bed voidage (0.40), d_p is the average diameter of catalyst particles (64.4 μm), and u_L is the superficial liquid feed velocity (m s^{-1}). Based on the observed values of liquid holdup in a micro packed bed reactor of between 0.65 and 0.85, a value of 0.75 was assumed for liquid holdup (h_L) in the mm-scale packed bed reactor under investigation.³⁸ The criterion value of $15.9 > 1.0$ confirmed that

the catalyst bed was fully wetted, leading to a more stable hydrodynamic state and uniform 1,4-cyclohexanedione distribution around the catalyst particles in the mm-scale reactor when compared to a trickle bed reactor. A previous study using 165 μm catalyst particles for the oxidation of liquid organic feedstocks showed a non-significant influence of gravitational forces on the reactor performance,³¹ with all experiments in this study performed using a reactor aligned in a horizontal position.

The narrow residence time distribution is characteristic of plug flow reactors in addition to the uniformity of the reaction environment that ensures the same operating conditions for each reactant along the reactor. A previous study³¹ has shown that plug flow normally occurs for the flow ranges operating in our reactor system, with a reactor diameter (d_r) to particle diameter (d_p) ratio of $46.6 > 10$ confirming the absence of wall effects on the plug flow pattern.³⁸ The radial distribution of the substrate concentration in the reactor can be considered to be uniform for large d_r/d_p values of >25 .⁴⁰ The effects of axial gradients can be neglected based on the reactor length to particle diameter ratio (L_r/d_p) of $466 > 50$, which was also confirmed by the particle Peclet number ($Pe_{p,ax}$),⁴¹ as calculated by eqn (2).

$$\frac{1}{Pe_{p,ax}} = \frac{\varepsilon_b}{\tau_b ReSc} + \frac{0.45}{1+0.73(ReSc)} < 0.10 \quad (2)$$

where τ_b (1.58) is the tortuosity of the catalyst packed bed, Re is the Reynolds number, and Sc is the Schmidt number. The details are provided in the ESI.† The Peclet number value of $0.003 < 0.10$ confirms the absence of axial concentration gradients in the catalyst bed of the mm-scale flow reactor.

The mass transport limitations in heterogeneous catalytic reactors can alter the reaction rates, selectivity and even the reaction mechanism.^{42,43} However, in order to evaluate the external mass transport limitation between the bulk fluid stream and the external catalyst surface, the Mears criterion⁴⁴ is utilized as described by eqn (3).

$$\frac{-r_{\text{obs}} \rho_b r_p^n}{k_{LS} C_B} < 0.15 \quad (3)$$

where $-r_{\text{obs}}$ is the observed rate of reaction, ρ_b is the catalyst bed bulk density (250 kg m^{-3}), r_p is the particle radius ($32.4 \times 10^{-6}\text{ m}$), n is the order of reaction (assumed as first order), k_{LS} is the overall liquid–solid mass transfer coefficient (see the ESI†), and C_B is the concentration of 1,4-cyclohexanedione in tetraethylene glycol dimethyl ether. The Mears criterion value of $7.90 \times 10^{-6} < 0.15$ confirms the absence of a concentration gradient between the bulk liquid feed and the catalyst surface.

The absence of intraparticle (internal) mass transfer limitation was verified by using the Weisz–Prater criterion⁴⁵ which represents the ratio of the reaction rate to the rate of diffusion in pores, as given by eqn (4).



$$C_{WP} = \frac{-r_{obs} \rho_b r_p^2}{D_{eff} C_{AS}} < 0.3 \quad (4)$$

where C_{AS} is the 1,4-cyclohexanedione concentration on the catalyst surface which can be assumed to be equivalent to the bulk concentration (C_B) in the absence of external mass transfer limitations, and D_{eff} is the effective diffusivity of 1,4-cyclohexanedione inside the liquid-filled pores of catalyst particles (see the ESI†). Apart from lower bulk diffusivity in liquid reaction systems, the effective diffusivity is influenced by liquid phase non-idealities, high affinity of diffusing species on the catalyst surface, molecule size comparable to the pore size, and adsorption phenomena.^{46–52} The Weisz–Prater criterion value of $0.20 < 0.3$ suggests the absence of pore diffusion limitation for a reaction order of 2 and lower.⁵³

These results suggest that the liquid-phase dehydrogenation reaction is performed in the kinetic regime under the investigated conditions with no transport (extra-particle and intra-particle diffusion) limitations.

3.1. Continuous dehydrogenation of 1,4-cyclohexanedione

For continuous flow (single-pass mode) liquid-phase dehydrogenation of 1,4-cyclohexanedione, the results are shown in Table S1 (see the ESI†) for 34 experiments designed by using D-optimal methodology. All the experiments were performed over 10 wt% Pd/C catalyst packed in a mm-scale structured multichannel reactor in a randomized order to avoid experimental bias, with three central point experiments showing that results were reproducible, with deviations between each run within an experimental error of $\pm 2.9\%$.

The experimental results (Table S1, see the ESI†) were analysed and quadratic models were developed using eqn (5) for conversion (Y_1) of 1,4-cyclohexanedione, selectivity (Y_2) for hydroquinone, and pressure drop (Y_3) in terms of temperature (X_1), nitrogen flow (X_2), liquid feed flow (X_3), and substrate concentration (X_4).

$$Y_i = \beta_0 + \sum_{i=1}^k \beta_i X_i + \sum_{i=1}^k \beta_{ii} X_i^2 + \sum_{i < j} \beta_{ij} X_i X_j \quad (5)$$

where Y_i is the response, β_0 is the intercept constant term, and β_i , β_{ii} and β_{ij} are the linear, square, and interaction regression coefficients, respectively. Experimental data were fitted to the models using a partial least squares (PLS) method followed by model refinement with a statistical analysis. Each response function was analysed for data distribution using histograms. A logarithmic transformation was applied to determine conversion and pressure drops, whereas a negative logarithmic transformation was used to calculate selectivities for a normal distribution of data.

The regression coefficient of quadratic models and standard error and P -values are given in Table 1. The model significance of each response function was evaluated through P -values, with a P -value of < 0.05 indicating that the coeffi-

Table 1 Regression coefficient of models for continuous dehydrogenation

Model term	Coefficient estimate	Standard error	P
(a) Conversion, $X(Y_1)$			
Constant	1.35	0.04	5.11×10^{-24}
X_1	0.36	0.02	5.65×10^{-15}
X_2	0.12	0.02	2.49×10^{-6}
X_3	-0.35	0.02	4.74×10^{-16}
X_4	5.94×10^{-3}	0.02	0.76
X_1^2	-0.18	0.03	6.73×10^{-6}
$X_1 \times X_2$	-0.11	0.02	2.31×10^{-6}
$X_1 \times X_3$	7.40×10^{-2}	0.02	5.30×10^{-4}
(b) Selectivity, $S(Y_2)$			
Constant	0.44	0.07	3.28×10^{-6}
X_1	-0.19	0.04	2.03×10^{-5}
X_2	0.03	0.04	0.50
X_3	0.13	0.04	2.04×10^{-3}
X_4	-6.97×10^{-2}	0.04	0.08
X_3^2	-0.32	0.07	6.31×10^{-5}
$X_1 \times X_3$	0.15	0.04	3.91×10^{-4}
(c) Pressure drop, $\Delta P(Y_3)$			
Constant	0.73	0.05	2.71×10^{-14}
X_1	-0.01	0.02	0.58
X_2	0.19	0.02	7.63×10^{-9}
X_3	0.16	0.02	5.29×10^{-8}
X_4	-6.87×10^{-3}	0.02	0.76
X_2^2	-8.80×10^{-2}	0.04	0.02
X_3^2	-9.52×10^{-2}	0.04	0.03
$X_1 \times X_3$	4.59×10^{-2}	0.02	0.04

X_1 = temperature (T , °C), X_2 = nitrogen flow (F_G , mL min⁻¹), X_3 = liquid feed flow (F_L , mL min⁻¹), and X_4 = substrate concentration (C_0 , wt%).

cient influenced the response function significantly, whilst a P -value of 0.05 indicated a non-significant effect. Additionally, a positive coefficient value was considered to correspond to a synergistic effect, whilst a negative value indicated an antagonistic effect of the factor on the selected response.

The summary of fit ($R^2 > 0.5$, $Q^2 > 0.5$, model validity > 0.25 , and reproducibility > 0.5) was used as a criterion to measure the quality of the model fit and its potential for prediction. As shown in Fig. 2, R^2 values of > 0.75 indicated a

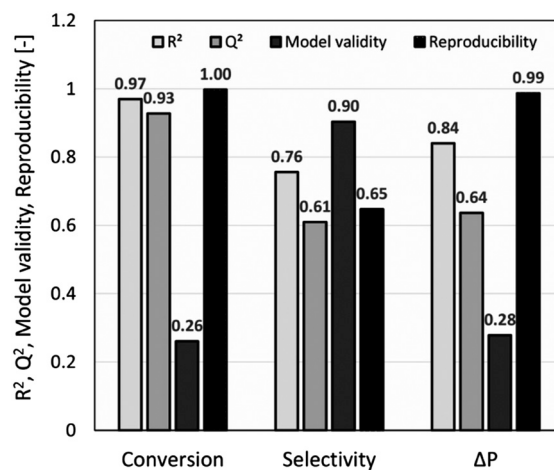


Fig. 2 Summary of fit for continuous dehydrogenation reaction of 1,4-cyclohexanedione.



good fit with a sufficiently precise description of experimental data to the models. However, due to several factors influencing a chemical reaction, a lower R^2 of ~ 0.7 was also considered acceptable,²⁷ whilst Q^2 values of >0.50 confirmed the good predictive capability for all models. Model diversity was probed using validity values of >0.25 , which confirmed the absence of statistically significant problems.⁵⁴ The high reproducibility values (>0.5) proved that the variation of replicates was less than the overall variation of the response function. For conversion and pressure drop, the model validity values were lower due to very high reproducibility values close to 1.0.⁵⁵

The significance of the model and model terms was evaluated using P -value (<0.05) and analysis of variance (ANOVA) at the 95% confidence level. Finally, all model predictions were then validated experimentally. ANOVA data shown in Table 2 reveal that the models are statistically significant at the 95% confidence level. The lack of fit (LoF) was calculated from the pure error and its residual. A high F -value implies that the lack of fit is non-significant relative to the pure error which suggests that the developed models are valid with good predictability. The statistical significance of the models was checked by comparing the values of the term “RSD \times sqrt($F(\text{crit})$)” with “regression-SD” where lower first values for all responses confirm that the models were significant at the

5% level. Lack of fit was non-significant for all models as confirmed by larger values for SD-pe \times sqrt($F(\text{crit})$) = 1.0281 than for SD-LoF. Fig. S2 (ESI[†]) reveals that the predicted values of the models were in good agreement with observed values, which confirmed that the factors are successfully correlated with the responses in the developed models.

The understanding of the dehydrogenation process was developed by studying the influence of a series of operating parameters on process functions, *i.e.* conversion, selectivity, and pressure drop.

3.1.1. Dehydrogenation of 1,4-cyclohexanedione. The influence of temperature and nitrogen flow on the catalytic dehydrogenation of 10 wt% 1,4-cyclohexanedione is shown as response surface plots in Fig. 3(a–d) for liquid flows of 0.10, 0.20, 0.40 and 0.50 mL min⁻¹ (0.7, 1.4, 2.7, 3.3 m³ m⁻² h⁻¹ at STP, respectively). With the variation in operating parameters, the conversion values ranged from 79.1% to 0.9%, with conversion rates decreasing with increasing liquid flow from 0.1 to 0.5 mL min⁻¹, which is caused by the shorter residence time of 1,4-cyclohexanedione in the catalyst bed. Increasing temperature showed an overall positive influence on substrate conversion levels due to the endothermic nature of the reaction.⁵⁶ The highest conversion peak was found in the temperature region of 220–230 °C for all liquid feed flow rates, suggesting the presence of optimal operating

Table 2 Analysis of variance (ANOVA) of the fitted model for continuous dehydrogenation

Source	DF	SS	MS (variance)	F	P	SD
(a) Conversion, $X(Y_1)$						
Total	34	58.14	1.71			
Constant	1	47.4	47.4			
Total corrected	33	10.74	0.33			0.57
Regression	7	10.42	1.49	120.6	0	1.2
Residual	26	0.32	1.24×10^{-2}			0.1
Lack of fit (LoF)	24	0.32	1.33×10^{-2}	18.61	0.05	0.1
Pure error (pe)	2	1.43×10^{-3}	7.16×10^{-4}			0.03
RSD \times sqrt($F(\text{crit})$) = 0.17						
SD-pe \times sqrt($F(\text{crit})$) = 0.12						
(b) Selectivity, $S(Y_2)$						
Total	34	5.69	0.17			
Constant	1	0.6	0.6			
Total corrected	33	5.09	0.15			0.39
Regression	6	3.85	0.64	13.91	0	0.8
Residual	27	1.24	4.61×10^{-2}			0.21
Lack of fit (LoF)	25	1.14	4.54×10^{-2}	0.84	0.68	0.21
Pure error (pe)	2	0.11	5.43×10^{-2}			0.23
RSD \times sqrt($F(\text{crit})$) = 0.34						
SD-pe \times sqrt($F(\text{crit})$) = 1.03						
(c) Pressure drop, $\Delta P(Y_3)$						
Total	34	12.8	0.38			
Constant	1	10.27	10.27			
Total corrected	33	2.54	7.68×10^{-2}			0.28
Regression	7	2.13	0.3	19.5	0	0.55
Residual	26	0.14	1.56×10^{-2}			0.12
Lack of fit (LoF)	24	0.4	1.68×10^{-2}	17.3	0.06	0.13
Pure error (pe)	2	1.94×10^{-3}	9.72×10^{-4}			0.03
RSD \times sqrt($F(\text{crit})$) = 0.19						
SD-pe \times sqrt($F(\text{crit})$) = 0.14						

DF = degree of freedom, SS = sum of squares, MS = mean square, SD = standard deviation, RSD = residual standard deviation, sqrt($F(\text{crit})$) = square root of critical F .



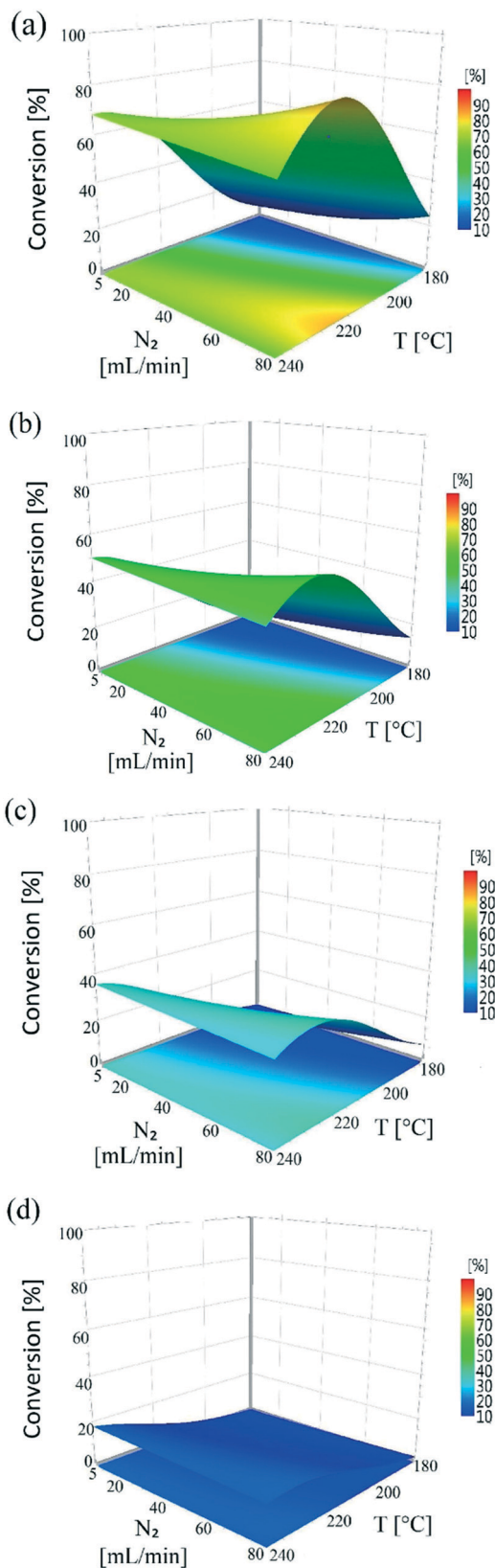


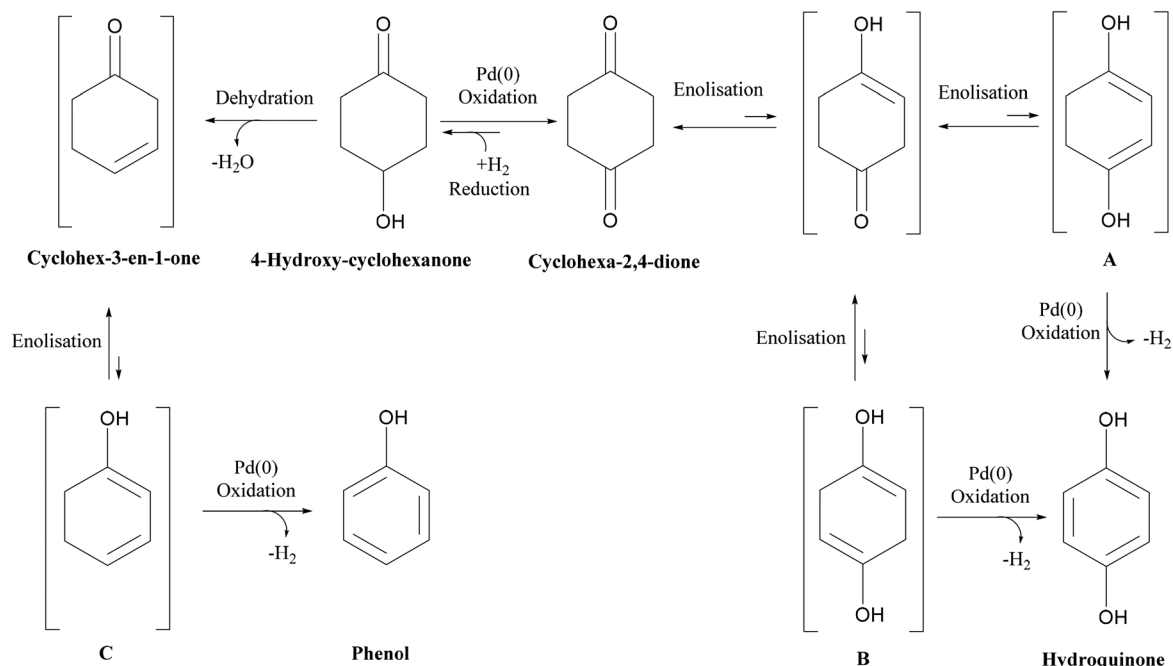
Fig. 3 Influence of temperature (180–240 °C) and nitrogen flow (5–80 mL min⁻¹, 33.3–566.7 m³ m⁻² h⁻¹ at STP) on conversion of substrate (10 wt%) for liquid feed flows of (a) 0.1 mL min⁻¹ (0.7 m³ m⁻² h⁻¹ at STP), (b) 0.2 mL min⁻¹ (1.4 m³ m⁻² h⁻¹ at STP), (c) 0.4 mL min⁻¹ (2.7 m³ m⁻² h⁻¹ at STP), and (d) 0.5 mL min⁻¹ (3.3 m³ m⁻² h⁻¹ at STP) in single-pass mode.

conditions. Moreover, this finding is in agreement with the optimal temperature range (180–260 °C) observed previously in a batch slurry reactor,⁸ with the DoE helping to narrow down the optimal temperature range in this flow reactor. The lowest conversion was obtained at the highest flow rate of 0.5 mL min⁻¹ and lowest temperature of 180 °C.

Nitrogen flow had a very minor but positive influence on conversion values, particularly at lower temperatures. This is likely due to the removal of H₂ of the reactor serving to drive the equilibrium of the dehydrogenation reaction towards hydroquinone formation. This situation is different from that of conventional hydrogenation/oxidation reactions where one of the gaseous reactants (hydrogen or oxygen) needs to diffuse from the gas to the liquid phase before it can reach the catalyst surface. This means that interactions between hydrogen (or oxygen) and the substrate on the catalyst surface are very important, with these types of catalytic hydrogenation/oxidation reactions strongly influenced by the hydrodynamics of the catalyst bed.⁵⁷ However, for the dehydrogenation reaction, 1,4-cyclohexanedione is already present in the liquid phase around the catalyst particles, which means that its distribution over the catalyst active sites is more uniform as the catalyst bed is fully wetted due to the presence of strong capillary forces. Moreover, changing the substrate concentration levels (1, 5, and 10 wt%) resulted in a non-significant effect on conversion rate as confirmed by a *P*-value of >0.05 (Fig. S3, ESI†). The results clearly indicate that it is not possible to obtain complete conversion of 1,4-cyclohexanedione in a single pass. The maximum conversion per pass was found to be 79.1% under the operating conditions of *T* = 240 °C, *F_L* = 0.1 mL min⁻¹, *F_G* = 45 mL min⁻¹ and *C_o* = 10 wt% but at the cost of lower selectivity of 91.9%. This result highlights the importance of finding an operating window to obtain maximum conversion while maintaining a selectivity of >99% at the same time.

3.1.2. Selectivity for formation of hydroquinone. The influence of operating conditions on the selectivity for hydroquinone was found to range from 91.9% to 99.8% under the investigated conditions. Scheme 1 shows the reactions occurring during the dehydrogenation process with hydroquinone, 4-hydroxycyclohexanone and phenol identified as products in all the 1,4-cyclohexanedione dehydrogenation experiments. The major reaction pathway for the conversion of 1,4-cyclohexanedione to hydroquinone is likely to proceed *via* an enolization pathway to afford bis-enols A and B that then undergo Pd(0)-mediated dehydrogenation to afford hydroquinone. The hydrogen generated from dehydrogenation of bis-enols A and B may then be used for the Pd(0)-mediated reduction of one of the keto groups of cyclohexa-1,4-dione to afford 4-hydroxycyclohexanone. Thermal dehydration of 4-hydroxycyclohexanone can then occur to afford cyclohex-3-en-1-one that can then enolise to afford bis-enol C which then undergoes Pd(0)-mediated dehydrogenation to afford phenol. The influence of substrate concentration (1–10 wt%) and nitrogen flow (5–80 mL min⁻¹, 33.3–566.7 m³ m⁻² h⁻¹ at STP) on the selectivity of the dehydrogenation reaction was negligible (see response surface plots displayed in Fig. S4





Scheme 1 Reaction schematic for dehydrogenation of 1,4-cyclohexanedione and formation of 4-hydroxycyclohexanone and phenol by-products.

and S5, ESI†). Capillary forces dominate viscous and gravitational forces in packed beds containing catalyst particles $<200\ \mu\text{m}$,³⁹ resulting in a thicker liquid layer around the catalyst particles. Nitrogen flow occurs preferentially through the voids available around the catalyst particles and as a consequence had no significant influence on selectivity.

Temperature (180–240 °C) and liquid feed flow (0.1–0.5 mL min⁻¹, 0.7–3.3 m³ m⁻² h⁻¹ at STP) showed a strong influence on selectivity as shown by the *P*-values (<0.05) of regression coefficients. Fig. 4 shows that the selectivity for hydroquinone declined with increasing temperature at lower liquid feed flow rates, which is likely linked to the residence time of 1,4-cyclohexanedione (and 4-hydroxycyclohexanone) in the catalyst bed. An increase in liquid feed flow from 0.1 mL min⁻¹

(235 °C, 5 wt% and 5 mL min⁻¹) to 0.2 mL min⁻¹ (240 °C, 5 wt% and 5 mL min⁻¹) results in a significant improvement in selectivity from 91.9% to 99.4% but at the price of a drop in conversion values from 79.1% to 61.2%. The results clearly show a wide operating window to obtain $>99\%$ selectivity.

3.1.3. Pressure drop. The influence of operating parameters on the variation of pressure drop was also investigated. The pressure drop was found to be strongly dependent on the liquid feed rate (5–80 mL min⁻¹, 33.3–566.7 m³ m⁻² h⁻¹ at STP) and nitrogen flow (0.1–0.5 mL min⁻¹, 0.7–3.3 m³ m⁻² h⁻¹ at STP), as shown in the response surface plot in Fig. 5. Temperature and substrate concentration appeared to be non-significant factors, as shown in the contour plot in Fig.

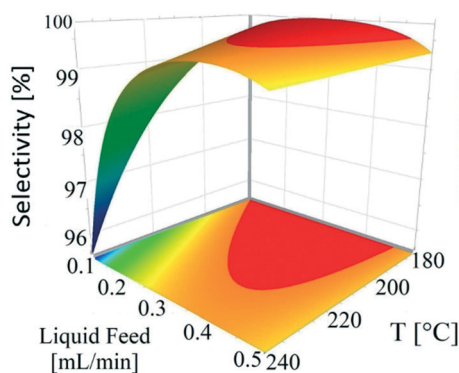


Fig. 4 Influence of temperature (180–240 °C) and liquid feed flow (0.1–0.5 mL min⁻¹, 0.7–3.3 m³ m⁻² h⁻¹ at STP) on the conversion and selectivity of 1,4-cyclohexanedione for a fixed nitrogen flow (40 mL min⁻¹, 266.4 m³ m⁻² h⁻¹ at STP) and substrate concentration (10 wt%) in single-pass mode.

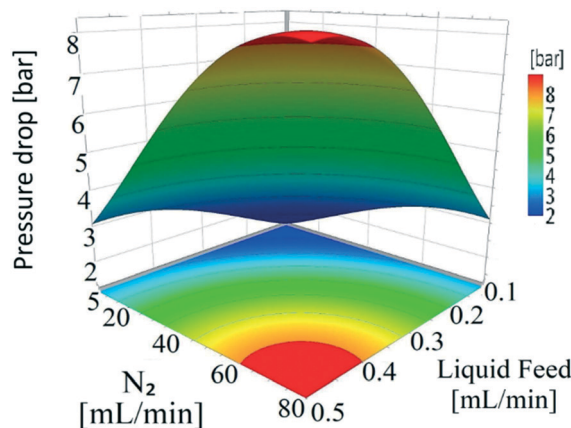


Fig. 5 Influence of nitrogen flow (5–80 mL min⁻¹, 33.3–566.7 m³ m⁻² h⁻¹ at STP) and liquid feed flow (0.1–0.5 mL min⁻¹, 0.7–3.3 m³ m⁻² h⁻¹ at STP) on the pressure drop for a substrate concentration of 1 wt% at 220 °C, in single-pass mode.



S6 (ESI[†]). Channel packing of fine catalyst particles in this type of fixed bed reactors is known to affect pressure drops,⁵⁸ so replicate experiments (N28, N29, and N30) were carried out using different catalyst packings over three different days. These replicate experiments at the centre point revealed reproducible pressure drop values (4.9 ± 0.4 bar), indicating that the pressure drop in these dehydrogenation reactions were not affected by the catalyst packing procedure.

3.2. Influence of channel arrangement and time on stream composition

The mm-scale structured reactor used in this study is much smaller in size and throughput when compared to conventional batch reactors; however, the throughput of the structured reactor can be increased by numbering-up mm-scale parallel channels.¹⁹ The time required to reach >98% hydroquinone yield in semi-continuous mode was 9 h, with reaction time being potentially reduced for a fixed reaction volume being achieved through increasing the number of mm-scale channels employed.

The reactor channels can be arranged in series to achieve higher yield, but this comes at a cost because of the need to use a large number of channels to drive conversion from 90% to >99%, caused by increasingly lower conversions per pass (see Fig. 7). For a recycling mode, the channels could potentially be arranged in series to increase reactor conversion per pass; however, the hydrogen produced in one channel may influence the selectivity in the next channel. To study the influence of produced hydrogen on side reactions, experiments were performed by connecting two channels in series, with and without intermediate gas removal, under operating conditions of $T = 230$ °C, 210 mg catalyst, back pressure = 1.5 bar, nitrogen flow rate = 35 mL min^{-1} ($233.1 \text{ m}^3 \text{ m}^{-2} \text{ h}^{-1}$ at STP), liquid feed flow rate = 0.20 mL min^{-1} ($1.4 \text{ m}^3 \text{ m}^{-2} \text{ h}^{-1}$ at STP), and substrate concentration = 5 wt%.

As shown in Fig. 6(a), two channels were connected with intermediate gas removal in a gas-liquid (G-L) separator, with a fresh nitrogen feed (35 mL min^{-1} , $233.1 \text{ m}^3 \text{ m}^{-2} \text{ h}^{-1}$ at STP) then introduced into the second channel. At the outlet of the first channel, the conversion of 1,4-cyclohexanedione was found to be $59.8 \pm 2.9\%$, which increased to $78.3\% \pm 2.6\%$ in the second channel, with the selectivity for hydroquinone maintained at >99% for both channels. However, when the product of the first channel was directly introduced into the second channel (no gas removal step, Fig. 6b), and whilst the selectivity in the first channel was maintained at >99%, the selectivity in the second channel decreased to $82.3 \pm 2.1\%$ due to the presence of hydrogen in the feed resulting in the formation of 4-hydroxycyclohexanone. Therefore, the relatively high substrate conversion level ($84.7 \pm 2.1\%$) observed in the second channel is associated with the formation of 4-hydroxycyclohexanone and phenol side products arising from the unwanted hydrogenation pathway.

The catalyst maintained its stability for conversion and selectivity in the dehydrogenation reaction over the 8 h reaction



Fig. 6 Influence of intermediate gas (nitrogen and hydrogen) on activity and selectivity for the dehydrogenation of 1,4-cyclohexanedione in two-channels-in-series in continuous mode (a) with intermediate hydrogen removal and (b) without hydrogen removal.

period (see Fig. 6). These conversion values suggest that the dehydrogenation reaction reaches steady-state conditions in

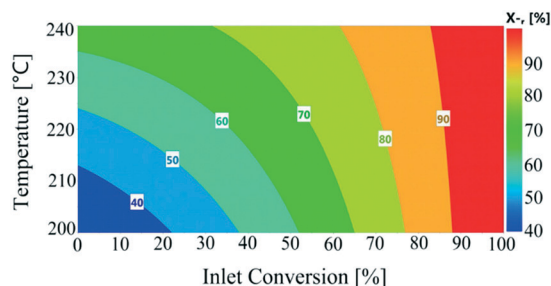


Fig. 7 Influence of reactor inlet conversion (0–100%) and temperature (200–240 °C) on reactor outlet conversion in recycle mode with substrate concentration of 5 wt% and nitrogen flow of 45 mL min^{-1} ($299.7 \text{ m}^3 \text{ m}^{-2} \text{ h}^{-1}$ at STP).



Optimal conditions for the developed models were determined using MODDE to generate a sweet spot plot for these transformations.⁶⁰ Fig. 8 shows the sweet spot plot obtained through RSM plots using MODDE, highlighting the process window where the reactor can be operated to meet the specified targets. The bright green area in the plot indicates the sweet spot where both objectives (conversion >40%, selectivity >99%) are met and the blue area indicates where only one target is fulfilled. A 4D contour plot for the sweet spot is shown in Fig. S12 (see the ESI†), indicating the sweet spots under the investigated conditions. A white area was identified at low liquid flow (0.10 mL min⁻¹, 0.7 m³ m⁻² h⁻¹ at STP) where no objective was met and no sweet spot was identified for 0.50 mL min⁻¹ (3.3 m³ m⁻² h⁻¹ at STP) liquid feed flow for a temperature range of 180–240 °C, nitrogen flow range of 5–85 mL min⁻¹ (33.3–602.1 m³ m⁻² h⁻¹ at STP) and substrate concentration range of 1–10 wt%.

Within the identified optimal operating window, the reactor also requires a set point where the response remains insensitive to variation in a reasonable range of operating factors, described as a robust set-point. Based on the sweet spot plots, a criterion of 50% conversion and 99% selectivity was selected as target values for establishing an optimal robust set-point. Robustness analyses were carried out to find the robust set-point among the optimal set-points. A robust set-point was identified at a temperature of 231.4 °C, 69.3 mL min⁻¹ (464.5 m³ m⁻² h⁻¹ at STP) nitrogen flow, 0.21 mL min⁻¹ (1.4 m³ m⁻² h⁻¹ at STP) liquid feed flow and a concentration of 9.28 wt% 1,4-cyclohexanedione, which was predicted to afford 51.9% conversion and 99.3% selectivity with a pressure drop of 4.8 bar. This dehydrogenation model was validated by experimental testing using the robust set-point parameters, which gave conversion, selectivity and pressure drop values of 53.6%, 99.1% and 5.3 bar, which were 1.7%, 0.2% and 0.8 bar different from the predicted values, respectively.

The final step in the process development was to establish optimal control ranges of operating conditions within which



Fig. 8 Sweet spot plot based on objectives of >40% conversion and >99% selectivity in single-pass mode for varying temperature (180–240 °C) and liquid feed flow (0.1–0.5 mL min⁻¹, 0.7–3.3 m³ m⁻² h⁻¹ at STP) at fixed nitrogen flow (40 mL min⁻¹, 266.4 m³ m⁻² h⁻¹ at STP) and substrate concentration (5 wt%).

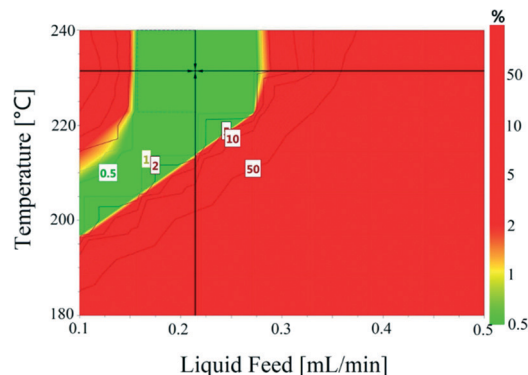


Fig. 9 Design space for the conversion of 1,4-cyclohexanedione in single-pass mode as a function of temperature (180–240 °C) and liquid feed flow (0.1–0.5 mL min⁻¹, 0.7–3.3 m³ m⁻² h⁻¹ at STP). The green area is the operating window to meet the desired specification, with the red area indicating risk of failure.

the performance (conversion and selectivity) of the dehydrogenation reaction could be maximized. This was achieved by identifying the design space, which was defined as a region of operating conditions with the least probability of failure to achieve the desired process output in the form of conversion, selectivity and pressure drop, as part of a quality by design approach.⁶¹ Fig. 9 shows the design space generated by MODDE at the robust set-point with operating factors of temperature and liquid feed flow. Reactor conversion was assumed not to change while operating within the design space. The design space plots for 1,4-cyclohexanedione conversion as a function of nitrogen flow and substrate concentration are shown as Fig. S13 and S14 (see the ESI†), respectively, which enabled the development of strong process control procedures.

The aim of finding a robust set-point was to operate the reactor to achieve complete conversion (>99%) while keeping the selectivity >99% for a semi-continuous dehydrogenation process. Liquid phase semi-continuous dehydrogenation was carried out at a robust set-point at 231.4 °C temperature, 69.3 mL min⁻¹ nitrogen flow (464.5 m³ m⁻² h⁻¹ at STP), and 0.21 mL min⁻¹ (1.4 m³ m⁻² h⁻¹ at STP) liquid feed flow with an

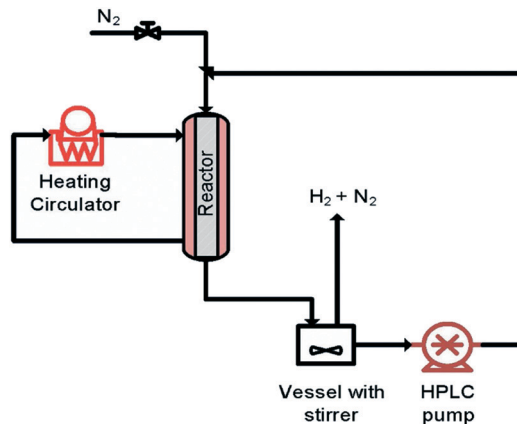


Fig. 10 The simplified scheme of semi-continuous dehydrogenation (recycle mode) of 1,4-cyclohexanedione.



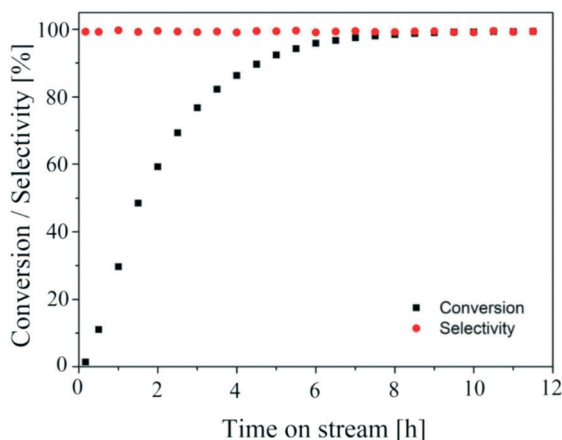


Fig. 11 Catalytic activity and selectivity of semi-continuous dehydrogenation (recycle mode) at a robust set-point, 231.4 °C, 69.3 mL min⁻¹ (464.5 m³ m⁻² h⁻¹ at STP) nitrogen flow, 0.21 mL min⁻¹ (1.4 m³ m⁻² h⁻¹ at STP) liquid feed flow and 9.28 wt% substrate concentration as a function of stream time (h).

initial concentration of 9.28 wt% 1,4-cyclohexanedione in tetraethylene glycol dimethyl ether as solvent. The simplified schematic of the set-up to carry out a semi-continuous dehydrogenation reaction in the same reactor is shown in Fig. 10. The reactor was packed with 210 mg of 10 wt% Pd/C catalyst, the catalyst was pre-wetted with substrate, and the reactor temperature was increased to 231.4 °C with a nitrogen flow rate of 69.3 mL min⁻¹ (464.5 m³ m⁻² h⁻¹ at STP). A liquid feed (9.28 wt% 1,4-cyclohexanedione) was then introduced at a rate of 0.21 mL min⁻¹ (1.4 m³ m⁻² h⁻¹ at STP) into the reactor from a feed vessel containing 20 mL initial feed volume. The feed vessel was equipped with a stirrer to enable homogenous mixing of a recycled product stream, with any gases being vented to the atmosphere. The samples were collected from the feed vessel with time for analysis by ¹H NMR spectroscopy and GC-MS. Fig. 11 shows the conversion of 1,4-cyclohexanedione and the selectivity for hydroquinone as a function of time on stream (h). The overall conversion is enhanced (1) by recycling of unconverted reactant and (2) by the removal of produced hydrogen in a G-L separator which removed the thermodynamic limitation. The selectivity for formation of hydroquinone was very high (>99%), which was maintained for ~11 h under the investigated conditions.

As discussed in the introduction, the liquid phase dehydrogenation of 1,4-cyclohexanedione in a batch slurry reactor previously resulted in a hydroquinone yield of 91.5%.⁸ In contrast, a hydroquinone yield of >98% and no side products (>99% selectivity) was observed in the mm-scale structured multichannel reactor used in this study, which was shown to function over a wide operating range.

4. Conclusions

A highly selective and continuous-flow process is successfully developed for the liquid-phase dehydrogenation of 1,4-

cyclohexanedione to hydroquinone over 10 wt% Pd/C catalyst in a scalable structured multichannel reactor. The design of experiment (DoE) methodology was utilized for experimental design to enhance process understanding and process optimization for the purpose of maximizing the yield. The experimental results were found to be in good agreement with the model's predicted values. Temperature and liquid feed flow strongly influenced the conversion and selectivity, with liquid feed and N₂ flows influencing the pressure drop significantly. Sweet spot plots were successfully used for multi-objective optimization, with optimum operating conditions found at a robust set-point of 231.4 °C, 69.3 mL min⁻¹ (464.5 m³ m⁻² h⁻¹ at STP) nitrogen flow, 0.21 mL min⁻¹ (1.4 m³ m⁻² h⁻¹ at STP) liquid feed flow, and 9.28 wt% 1,4-cyclohexanedione concentration. The continuous-flow process was successfully demonstrated for liquid-phase dehydrogenation in single-pass and recycle modes. The results proved that complete conversion is not obtained in a single pass per channel which might be due to thermodynamic or kinetic limitations. However, the conversion increased from 59.8% for one-channel to 78.3% for two-channels-in-series while maintaining high selectivity (>99%) with intermediate hydrogen removal. Without the intermediate H₂ removal step in the gas-liquid separator, the selectivity decreased to 82.3% in the second channel. Finally, the experiments in recycle mode demonstrated that almost complete conversion (>99%) of 1,4-cyclohexanedione was obtained for recycle mode dehydrogenation with very high selectivity (>99%) and yield (>98%).

Conflicts of interest

There are no conflicts to declare.

Acknowledgements

The authors acknowledge the EPSRC for funding the project "Terpene-based Manufacturing for Sustainable Chemical Feedstocks" EP/K014889/1. All the data of this study are available in the ESI.†

References

- 1 T. Letcher, J. Scott and D. A. Patterson, *Chemical Processes for a Sustainable Future*, Royal Society of Chemistry, Abingdon, U. K., 2014.
- 2 P. Imhof and J. C. van der Waal, *Catalytic Process Development for Renewable Materials*, Wiley VCH, Weinheim, Germany, 2013.
- 3 R. A. Sheldon and H. van Bekkum, *Fine Chemicals through Heterogeneous Catalysis*, Wiley, 2008.
- 4 P. M. Hudnall, in *Ullmann's Encyclopedia of Industrial Chemistry*, Wiley-VCH Verlag GmbH & Co. KGaA, 2000, DOI: 10.1002/14356007.a13_499.
- 5 F. Gokden and A. Lazzarotto, *Hydroquinone: Production, Uses, and Health Effects*, Nova Science Publishers, 2012.
- 6 N. N. Pozdeeva and E. T. Denisov, *Kinet. Catal.*, 2011, 52, 506.



- 7 S. C. Gad and T. Pham, in *Encyclopedia of Toxicology*, Academic Press, Oxford, 3rd edn, 2014, pp. 979–981, DOI: 10.1016/B978-0-12-386454-3.00855-1.
- 8 H. Krekeler and W. H. Muller, US4024196A, 1977.
- 9 A. T. Nielsen and W. R. Carpenter, *Org. Synth.*, 1965, 45, 25.
- 10 K.-K. Cheng, X.-B. Zhao, J. Zeng and J.-A. Zhang, *Biofuels, Bioprod. Biorefin.*, 2012, 6, 302–318.
- 11 A. A. Lapkin, P. K. Heer, P. M. Jacob, M. Hutchby, W. Cunningham, S. D. Bull and M. G. Davidson, *Faraday Discuss.*, 2017, 202, 483–496.
- 12 J. W. Zhang, Q. Q. Jiang, D. J. Yang, X. M. Zhao, Y. L. Dong and R. H. Liu, *Chem. Sci.*, 2015, 6, 4674–4680.
- 13 A. Cybulski, M. M. Sharma, R. A. Sheldon and J. A. Moulijn, *Fine Chemicals Manufacture: Technology and Engineering*, Elsevier Science, Amsterdam, The Netherlands, 1st edn, 2001.
- 14 J. Salaklang, V. Maes, M. Conradi, R. Dams and T. Junkers, *React. Chem. Eng.*, 2018, 3, 41–47.
- 15 S. Schwolow, A. Neumüller, L. Abahmane, N. Kockmann and T. Röder, *Chem. Eng. Process.: Process Intensif.*, 2016, 108, 109–116.
- 16 E. Novakova, N. Winterton, K. Jarosch and J. Brophy, *Catal. Commun.*, 2005, 6, 586–590.
- 17 P. Kleinebudde, J. Khinast and J. Rantanen, *Continuous Manufacturing of Pharmaceuticals*, Wiley, 2017.
- 18 V. Hessel, *Chem. Eng. Technol.*, 2009, 32, 1655–1681.
- 19 J. Wegner, S. Ceylan and A. Kirschning, *Chem. Commun.*, 2011, 47, 4583–4592.
- 20 N. Kockmann, M. Gottsponer and D. M. Roberge, *Chem. Eng. J.*, 2011, 167, 718–726.
- 21 I. Rossetti and M. Compagnoni, *Chem. Eng. J.*, 2016, 296, 56–70.
- 22 A. Tanimu, S. Jaenicke and K. Alhooshani, *Chem. Eng. J.*, 2017, 327, 792–821.
- 23 Y. Su, Y. Zhao, F. Jiao, G. Chen and Q. Yuan, *AIChE J.*, 2011, 57, 1409–1418.
- 24 M. F. Nagiev, *The Theory of Recycle Processes in Chemical Engineering*, Pergamon, 1964.
- 25 Z. R. Lazic, *Design of Experiments in Chemical Engineering: A Practical Guide*, Wiley, 2006.
- 26 P. M. Murray, F. Bellany, L. Benhamou, D.-K. Bucar, A. B. Tabor and T. D. Sheppard, *Org. Biomol. Chem.*, 2016, 14, 2373–2384.
- 27 S. Soravia and A. Orth, in *Ullmann's Encyclopedia of Industrial Chemistry*, Wiley-VCH Verlag GmbH & Co. KGaA, 2000, DOI: 10.1002/14356007.e08_e01.pub2.
- 28 S. A. Weissman and N. G. Anderson, *Org. Process Res. Dev.*, 2015, 19, 1605–1633.
- 29 R. H. Myers, D. C. Montgomery and C. M. Anderson-Cook, *Response Surface Methodology: Process and Product Optimization Using Designed Experiments*, Wiley, 2016.
- 30 D. V. Bavykin, A. A. Lapkin, S. T. Kolaczkowski and P. K. Plucinski, *Appl. Catal., A*, 2005, 288, 175–184.
- 31 P. K. Plucinski, D. V. Bavykin, S. T. Kolaczkowski and A. A. Lapkin, *Catal. Today*, 2005, 105, 479–483.
- 32 X. Fan, V. Sans, S. K. Sharma, P. K. Plucinski, V. A. Zaikovskii, K. Wilson, S. R. Tennison, A. Kozynchenko and A. A. Lapkin, *Catal. Sci. Technol.*, 2016, 6, 2387–2395.
- 33 X. L. Fan, M. G. Manchon, K. Wilson, S. Tennison, A. Kozynchenko, A. A. Lapkin and P. K. Plucinski, *J. Catal.*, 2009, 267, 114–120.
- 34 T. Moreno, J. Garcia-Serna, P. Plucinski, M. J. Sanchez-Montero and M. J. Cocero, *Appl. Catal., A*, 2010, 386, 28–33.
- 35 M. H. Aldahhan and M. P. Dudukovic, *AIChE J.*, 1996, 42, 2594–2606.
- 36 N. M. Márquez Luzardo, *Doctoral thesis*, Technische Universiteit Delft, 2010.
- 37 A. Faridkhou, J.-N. Tourvieille and F. Larachi, *Chem. Eng. Process.: Process Intensif.*, 2016, 110, 80–96.
- 38 J. A. Moulijn, M. Makkee and R. J. Berger, *Catal. Today*, 2016, 259, 354–359.
- 39 S. T. Sie, *Rev. Inst. Fr. Pet.*, 1991, 46, 501–515.
- 40 S. T. Sie and R. Krishna, *Rev. Chem. Eng.*, 1998, 14, 203–252.
- 41 B. H. Alsolami, R. J. Berger, M. Makkee and J. A. Moulijn, *Ind. Eng. Chem. Res.*, 2013, 52, 9069–9085.
- 42 C. Sievers, Y. Noda, L. Qi, E. M. Albuquerque, R. M. Rioux and S. L. Scott, *ACS Catal.*, 2016, 6, 8286–8307.
- 43 L. Rodríguez-García, R. Walker, E. Spier, K. Hungerbühler and F. Meemken, *React. Chem. Eng.*, 2018, 3, 55–67.
- 44 D. E. Mears, *Ind. Eng. Chem. Process Des. Dev.*, 1971, 10, 541–547.
- 45 G. Ertl, H. Knözinger and J. Weitkamp, *Handbook of heterogeneous catalysis*, VCH, Weinheim, 1997.
- 46 P. A. Ramachandran and R. V. Chaudhari, *Three-phase catalytic reactors*, Gordon and Breach Science Publishers, New York, 1983.
- 47 A. Chantong and F. E. Massoth, *AIChE J.*, 1983, 29, 725–731.
- 48 C. N. Satterfield and J. R. Katzner, in *Molecular Sieve Zeolites-II*, American Chemical Society, 1971, ch. 55, vol. 102, pp. 193–208.
- 49 B. D. Prasher, G. A. Gabriel and Y. H. Ma, *AIChE J.*, 1978, 24, 1118–1122.
- 50 C. N. Satterfield, C. K. Colton and W. H. Pitcher, *AIChE J.*, 1973, 19, 628–635.
- 51 J. M. Smith, *Chemical Engineering Kinetics*, McGraw-Hill, 1981.
- 52 C. N. Satterfield, *Mass transfer in heterogeneous catalysis*, M. I.T. Press, 1970.
- 53 P. B. Weisz, *Z. Phys. Chem.*, 1957, 11, 1–15.
- 54 J. Ermer and J. H. M. B. Miller, *Method Validation in Pharmaceutical Analysis: A Guide to Best Practice*, Wiley, 2006.
- 55 User Guide to MODDE - Umetrics, https://umetrics.com/sites/default/files/downloads/1/user_guide_to_modde_10.1.pdf, 2017.
- 56 J. M. Winterbottom and M. King, *Reactor Design for Chemical Engineers*, CRC Press, 2018.
- 57 N. Al-Rifai, F. Galvanin, M. Morad, E. H. Cao, S. Cattaneo, M. Sankar, V. Dua, G. Hutchings and A. Gavriilidis, *Chem. Eng. Sci.*, 2016, 149, 129–142.



- 58 A. Faridkhou, M. Hamidipour and F. Larachi, *Chem. Eng. J.*, 2013, **223**, 425–435.
- 59 G. P. Rangaiah and P. A. Bonilla-Petriciolet, *Multi-Objective Optimization in Chemical Engineering: Developments and Applications*, Wiley, 2013.
- 60 E. Castillo, *Process Optimization: A Statistical Approach*, Springer US, 2007.
- 61 C. Hakemeyer, N. McKnight, R. St. John, S. Meier, M. Trexler-Schmidt, B. Kelley, F. Zettl, R. Puskeiler, A. Kleinjans, F. Lim and C. Wurth, *Biologicals*, 2016, **44**, 306–318.

